Supporting Information

Zhiponova et al. 10.1073/pnas.1400203111

SI Methods

***Arabidopsis* Mutants and Transgenic Lines.** Single insertion lines in the promoter region of INCREASED LEAF INCLINATION1 BINDING BASIC HELIX–LOOP–HELIX 1 (IBH1)/basic helix–loop–helix 158 (bHLH158) and the exon region of IBH1-LIKE1 (IBL1)/bHLH159 have been genotyped: SALK 049177 (*ibh1*) and SALK 119457 (*ibl1*), respectively (Dataset S8). For generation of transgenic plants with overexpressed and endogenous levels of IBH1 and IBL1, the respective cDNAs were amplified by PCR from an *Arabidopsis* cDNA library and cloned into the Gateway entry vector pDONR221 (1). Constructs containing *pro35S::cDNA-GFP* and *procDNA::cDNA-GFP* translational fusions were generated in pK7FWG2,0 and pK7m34GW vectors, respectively, according to the manufacturer's instructions (Invitrogen). Binary vectors were introduced into *Agrobacterium tumefaciens* strain LBA4404 by electroporation and then transformed into wild-type *A. thaliana* (L.) Heynh (accession Columbia-0) or *brassinosteroid-insensitive1-5* (*bri1-5*) (2) plants by the floral dip method (3). Homozygous plants with single gene insertion were selected and assayed. The *p35S::IBL1-GFP* line 1 was used for RNA analysis followed by sequencing (RNA-Seq) and ChIP analysis followed by sequencing (ChIP-Seq).

Hypocotyl Measurement. Hypocotyls were photographed by a Nikon camera connected to a binocular Leica microscope MZ16 for a subsequent length measuring with the ImageJ software (4). Epidermal cells were imaged by a differential interference contrast microscope BX51 (Olympus), and their length was measured by ImageJ. The average values with SE, number of samples, and statistical Student's *t* test are given in the figures.

Total RNA Isolation. Three independent biological replicates (that is, material obtained from three different growth sets) were snap-frozen in N_2 and stored at −80 °C. Total RNA was extracted with the RNeasy Plant Mini Kit followed by DNaseI treatment (Qiagen). The RNA was subjected to DNaseI (Promega) treatment and tested by PCR to confirm the lack of genomic DNA contamination. cDNA was synthesized from 1 mg total RNA by means of SuperScript Reverse Transcriptase II (Invitrogen) with oligo-$dT_{12\text{-}18}$ as primer.

RNA-Seq. The mRNA-Seq libraries with biological duplicates were prepared with the Illumina mRNA-Seq Sample Preparation Kit (15008136; Illumina) according to the manufacturer's instructions. Of total RNA, 200 ng were hybridized two times to oligo-dT beads (Illumina). The poly(A)-enriched mRNA was fragmented by heating at 94 °C for 12 min in the fragmentation buffer (Illumina) followed by ethanol precipitation. The fragmented mRNA was added to 1× first-strand buffer (2.5 mM deoxynucleotide triphosphate, 10 mM DTT, RNaseOUT, random primers mix). After SuperScript II Reverse Transcriptase (Invitrogen) had been added, first-strand cDNA was synthesized at 25 °C for 10 min, 42 °C for 50 min, and 70 °C for 15 min. Second-strand cDNA was synthesized in 1× second-strand buffer (Illumina) and purified by Agencourt AMPure (Beckman Coulter). After end repair and A-base addition, adapters were ligated with the Illumina multiplexing system. Different indexes were used for each library. The ligated fragments were purified with Agencourt AMPure (Beckman Coulter) followed by PCR amplification (18 cycles), and the PCR products were also purified with Agencourt AMPure (Beckman Coulter). Library DNA was checked for concentration and size distribution in a Bioanalyzer (Agilent) before being subjected to Illumina GA sequencing with the Nucleic Acid Shared Resource-Illumina GAII Core (The Ohio State University Comprehensive Cancer Center). For the Illumina multiplexing system, the overall procedure was according to the manufacturer's instructions (TruSeq RNA Sample Preparation Guide, 15008136; Illumina). The given short reads were mapped with TopHat on Galaxy (5) with TAIR9. The differentially expressed genes were indicated as false discovery rate (FDR) < 0.05 with CuffDiff on Galaxy. For RNA-Seq validation, quantitative RT-PCR was run to estimate gene transcript levels in the respective IBH1 and IBL1 gain- and loss-of-function plants.

ChIP-Seq. ChIP was done as described previously (6). Briefly, for each biological repeat, ∼180 mg tissue [that is, 60 mg per input (not antibody-treated control), GFP, and IgG immunoprecipitations] was fixed in buffer A (0.4 M sucrose, 10 mM Tris·HCl, pH 8.0, 1 mM EDTA, 1% formaldehyde) for 10 min under vacuum conditions. Glycine was added at a final concentration of 0.1 M, and incubation was continued for an additional 10 min. Fixed tissue was washed in distilled water, frozen in liquid N_2, and ground in liquid N_2 followed by nuclear isolation with the Plant Nuclei Isolation/Extraction Kit according to the manufacturer's instructions (Sigma-Aldrich). Nucleus-enriched extracts were resuspended in 100 μL lysis buffer (50 mM Hepes, pH 7.5, 150 mM NaCl, 1 mM EDTA, 1% Triton X-100, 0.1% deoxycholate, 0.1% SDS) and plant proteinase inhibitor mixture (Sigma-Aldrich) followed by sonication with a Bioruptor (Diagenode) to ∼300 bp of average fragment size (estimated by agarose electrophoresis).

The sonicated nuclear extracts were precleared with 30 μL Dynabeads without antibody for 120 min at 4 °C and subsequently immunoprecipitated with 1 μL anti-GFP antibody (ab290; Abcam) or 1 μL anti-IgG antibody (ab37415; Abcam) as a control at 4 °C overnight. Dynabeads protein A (Invitrogen) were added and incubated for 4 h to precipitate the chromatin complexes. After incubation, beads were washed two times with each buffer: lysis buffer, LNDET buffer of 0.25 M LiCl, 1% Nonidet P-40, 1% deoxycholate, and 1 mM EDTA, and Tris·EDTA buffer. The washed beads and input fraction were resuspended in elution buffer (1% SDS, 0.1 M $NaHCO_3$, 0.2 mg/mL proteinase K, 1 mM DTT) and incubated at 65 °C overnight for reverse cross-link. After RNase treatment, the immunoprecipitated and input DNA were purified with the PCR Purification Kit (Qiagen). The ChIP experiments were done in replicate, from which the means and standard deviations were calculated.

The ChIP-Seq library was prepared as described previously (7). ChIP DNA, pooled from three independent ChIP experiments, were end-repaired and supplemented with A base followed by ligation with adapters, Mltplx_Short, and Mltplx_Long (Dataset S8). Gel-purified ligated libraries were amplified by Phusion Taq (New England Biolabs) for 18 cycles with MltplxPCR1.0 and two different primers (PCR2.0_indx2 for *p35S::IBH1-GFP* or PCR2.0_indx6 for Columbia-0). Illumina GA sequencing was done with the Nucleic Acid Shared Resource-Illumina GAII Core (The Ohio State University Comprehensive Cancer Center). The given short reads were aligned to the *Arabidopsis* genome (TAIR9) by Bowtie with default parameters, except that three mismatches were allowed. The uniquely aligned data were analyzed with the model-based analysis of ChIP-Seq (MACS) (1.4.0β) (8) to find peaks ($P < 10^{-5}$; no duplicated fragments allowed). Target genes were defined as statistically significant when binding peaks appeared on their genic and/or within 3-kb

upstream region(s) according to the TAIR9 annotation and were found by means of BEDTools (9). We applied the same analysis method for publicly available PHYTOCHROME-INTERACTING FACTOR4 (PIF4) ChIP-Seq data (GSE35315), and BRASSINAZOLE-RESISTANT1 (BZR1) ChIP followed by microarray analysis (GSE23774) (6). Peak colocalization was analyzed with R version 2.15.0 (http://www.r-project.org) and drawn with the ggplot2 package (10).

To test binding of IBH1 and IBL1 to helix–loop–helix/bHLH targets, ChIP assay followed by quantitative PCR (ChiP-qPCR) was run on ChIP DNA from plants expressing endogenous levels of IBH1 and IBL1 (*pIBH1::IBH1-GFP* and *pIBL1::IBL1-GFP*, respectively). For the ChIP-Seq validation of random IBH1 binding peaks, ChIP-qPCR was run on DNA from plants with increased levels of IBH1 (*p35S::IBH1-GFP*).

PCR Analysis. cDNA or ChIP-derived DNA was used as a template for qRT-PCR or ChIP-qPCR amplification, respectively, in an iCycler iQ detection system with Optical System Software (v3.0a; Bio-Rad) with the intercalation dye SYBR Green I (Invitrogen) as the fluorescent reporter and Platinum Taq Polymerase (Invitrogen). Primers were designed to generate fragments between 80 and 150 bp by means of QuantPrime for cDNA (11) and Primer 3 (12, 13) (http://primer3.sourceforge.net/) for ChIP-DNA (Dataset S8). At least three biological replicates were performed for each sample. The translation initiation factor *EF1* was used to normalize the obtained values. Amplification conditions were 2 min denaturation at 94 °C and 40–45 cycles at 94 °C for 15 s, 57 °C for 20 s, and 72 °C for 20 s followed by a final extension step at 72 °C for 5 min.

Motif-Based Sequence and FunCat Analysis. For motif-based sequence analysis, the MEME-ChIP (http://meme.sdsc.edu/meme/cgi-bin/meme-chip.cgi) was used with default parameter sets. To limit the peak abundance, default criteria were applied; only peaks with an FDR < 0.01 were chosen, and 100-bp sequences around the peak centers were selected. To explore the features of target genes, FunCat enrichment was analyzed with the MIPS web site (http://mips.helmholtz-muenchen.de/proj/funcatDB/search_main_frame.html). The enriched FunCats ($P < 0.05$) are indicated for each case.

Data Comparisons. Proteins were aligned with the PRALINE program (www.ibi.vu.nl/programs/pralinewww/). The Venn Selector tool in the Bio-Analytic Resource for Plant Biology (http://bar.utoronto.ca/welcome.htm) was used to find overlaps in the datasets.

Statistical Analysis. For statistical analyses, Student's *t* and Fisher exact tests were used, and significant values ($P < 0.05$) are indicated for each experiment. In the case of RNA-Seq analyses, the differentially expressed genes were indicated as FDR < 0.05 with CUFFDIFF on Galaxy. The statistical values in the ChIP-Seq datasets were calculated with MACS (9) (1.4.0β).

Yeast Two-Hybrid Assay. The yeast clones for IBH1 (pDest-AD053G03 and pDest-DB053G03) and PIF4 (pDest-AD093F11 and pDest-DB093F11) were obtained from the *Arabidopsis* Biological Research Center (abrc.osu.edu). The plasmids containing IBH1 and PIF4 in the pDest-AD and pDest-DB vectors were cotransformed into yeast strain pJ694a (14) and plated on synthetic complete medium (SC, Fisher DF0335-15-9) lacking the amino acids leucine (Leu) and tryptophan (Trp). As positive controls, Gal4AD-AtDIV1 and Gal4DBD-AtDIV1 were used (15). Colonies were screened for growth on SC medium lacking: (i) Leu, Trp; (ii) Leu, Trp, histidine (His); and (iii) Leu, Trp, His, adenine (Ade). In the absence of the original empty pDest-AD vector, clone pDest-DB053G03 was transformed alone into PJ69.4a, plated on SC medium without Trp, and screened for growth on SC medium lacking: (i) Trp; (ii) Trp, His; and (iii) Trp, His, Ade.

Bimolecular Fluorescence Complementation. The bimolecular fluorescence complementation constructs of IBH1 and PIF4 (16) were generated as previously described (17) in pK7m34GW destination vector (18). hGFP and tGFP constructs (19) were used as controls. *A. tumefaciens*-mediated transient transformation of *Nicotiana benthamiana* leaves was done as described (19) with minor modifications. In brief, *Agrobacterium* strains transformed with the bimolecular fluorescence complementation constructs were grown for 2 d in yeast extract broth medium and resuspended in infiltration buffer (10 mM MES, 10 mM $MgCl_2$, 0.1 mM acetosyringone) at the final OD_{600} value of one. In a similar way, the p19 protein of the tomato bushy stunt virus was used to suppress gene silencing. Before the leaf infiltration, 330 mL of each bacterial culture and p19 virus were mixed for a total volume of 990 mL and infiltrated into leaves of 4-wk-old *N. benthamiana* plants. Leaves were imaged 4 d after infiltration.

Accession Numbers. Sequence data from this article can be found in the *Arabidopsis* Genome Initiative of the GenBank/European Molecular Biology Laboratory databases under the following accession numbers: ACTIVATOR FOR CELL ELONGATION1 (ACE1; At1g68920), ACE2 (At1g10120), ACE3 (At3g23690), ACTIVATION-TAGGED-BRI1-SUPPRESSOR1–INTERACTING FACTOR1 (AIF1; At3g05800), AIF2 (At3g06590), AIF3 (At3g17100), AIF4 (At1g09250), HOMOLOG OF BRASSINOSTEROID-ENHANCED EXPRESSION2 (At4g36540), bHLH060 (At3g57800), bHLH074 (At1g10120), bHLH137 (At5g50915), bHLH146 (At4g30180), BZR2/BRI1-EMS-SUPPRESSOR1-INTERACTING MYC-LIKE PROTEIN1 (At5g08130), BR-INSENSITIVE2 (At4g18710), BR-INSENSITIVE1 (At4g39400), BZR1 (At1g75080), BZR2/BRI1-EMS-SUPPRESSOR1 (At1g19350), CRYPTOCHROME INTERACTING bHLH1 (At4g34530), CONSTITUTIVE PHOTOMORPHOGENIC DWARF (At5g05690), DELLA (RGA1/At2g01570, GAI/At1g14920, RGL1/At1g66350, RGL2/At3g03450, and RGL3/At5g17490), INTERACTING WITH IBH1 (At2g18300), LONG HYPOCOTYL IN FAR-RED REDUCED PHYTOCHROME SIGNALING1 (At1g02340), IBH1 (At2g43060), IBL1 (At4g30410), INDUCER OF CBP EXPRESSION1 (At3g26744), IAA-LEUCINE RESISTANT3 (At5g54680), FLOWERING BHLH4 (At2g42280), MITOGEN-ACTIVATED PROTEIN KINASE3 (At3g45640), MYELOBLASTOSIS FAMILY TRANSCRIPTION FACTOR-LIKE2 (At1g71030), OBP3-RESPONSIVE GENE2 (At3g56970), ORG3 (At3g56980), PHYTOCHROME RAPIDLY REGULATED1 (At2g42870), PIF4 (At2g43010), PIF5 (At3g59060), PIF1 (At2g20180), PACLOBUTRAZOL RESISTANCE 1 (At5g39860), PRE3/ACTIVATION-TAGGED-BRI1-SUPPRESSOR1 (At1g74500), PRE6 (At1g26945), POPEYE (At3g47640), P1R1 (At5g57780), P1R3 (At3g29370), TARGET OF MONOPTEROS5 (TMOS5; At3g25710), TMO5-like1 (At1g68810), and UP-BEAT1 (At2g47270). The *Zea mays* R protein accession number is GRMZM5G822829. All of the short sequence data generated as part of this study are deposited in the Gene Expression Omnibus (www.ncbi.nlm.nih.gov/geo/).

1. Karimi M, Inzé D, Depicker A (2002) GATEWAY™ vectors for *Agrobacterium*-mediated plant transformation. *Trends Plant Sci* 7(5):193–195.
2. Noguchi T, et al. (1999) Brassinosteroid-insensitive dwarf mutants of Arabidopsis accumulate brassinosteroids. *Plant Physiol* 121(3):743–752.
3. Clough SJ, Bent AF (1998) Floral dip: A simplified method for *Agrobacterium*-mediated transformation of *Arabidopsis thaliana*. *Plant J* 16(6):735–743.
4. Abràmoff M, Magalhães P, Ram S (2004) Image processing with ImageJ. *Biophotonics Int* 11(7):36–42.

5. Goecks J, Nekrutenko A, Taylor J; Galaxy Team (2010) Galaxy: A comprehensive approach for supporting accessible, reproducible, and transparent computational research in the life sciences. *Genome Biol* 11(8):R86.
6. Morohashi K, Xie Z, Grotewold E (2009) Gene-specific and genome-wide ChIP approaches to study plant transcriptional networks. *Methods Mol Biol* 553:3–12.
7. Morohashi K, et al. (2012) A genome-wide regulatory framework identifies maize *pericarp color1* controlled genes. *Plant Cell* 24(7):2745–2764.
8. Quinlan AR, Hall IM (2010) BEDTools: A flexible suite of utilities for comparing genomic features. *Bioinformatics* 26(6):841–842.
9. Zhang Y, et al. (2008) Model-based Analysis of ChIP-Seq (MACS). *Genome Biol* 9(9): R137.
10. Wickham H (2009) *ggplot2: Elegant Graphics for Data Analysis (Use R! Series)* (Springer, Berlin).
11. Arvidsson S, Kwasniewski M, Riaño-Pachón DM, Mueller-Roeber B (2008) QuantPrime—a flexible tool for reliable high-throughput primer design for quantitative PCR. *BMC Bioinformatics* 9:465.
12. Untergasser A, et al. (2012) Primer3—new capabilities and interfaces. *Nucleic Acids Res* 40(15):e115.
13. Koressaar T, Remm M (2007) Enhancements and modifications of primer design program Primer3. *Bioinformatics* 23(10):1289–1291.
14. James P, Halladay J, Craig EA (1996) Genomic libraries and a host strain designed for highly efficient two-hybrid selection in yeast. *Genetics* 144(4):1425–1436.
15. Machemer K, et al. (2011) Interplay of MYB factors in differential cell expansion, and consequences for tomato fruit development. *Plant J* 68(2):337–350.
16. de Lucas M, et al. (2008) A molecular framework for light and gibberellin control of cell elongation. *Nature* 451(7177):480–484.
17. Boruc J, et al. (2010) Functional modules in the *Arabidopsis* core cell cycle binary protein-protein interaction network. *Plant Cell* 22(4):1264–1280.
18. Karimi M, Bleys A, Vanderhaeghen R, Hilson P (2007) Building blocks for plant gene assembly. *Plant Physiol* 145(4):1183–1191.
19. Di Rubbo S, et al. (2013) The clathrin adaptor complex AP-2 mediates endocytosis of brassinosteroid insensitive1 in *Arabidopsis*. *Plant Cell* 25(8):2986–2997.

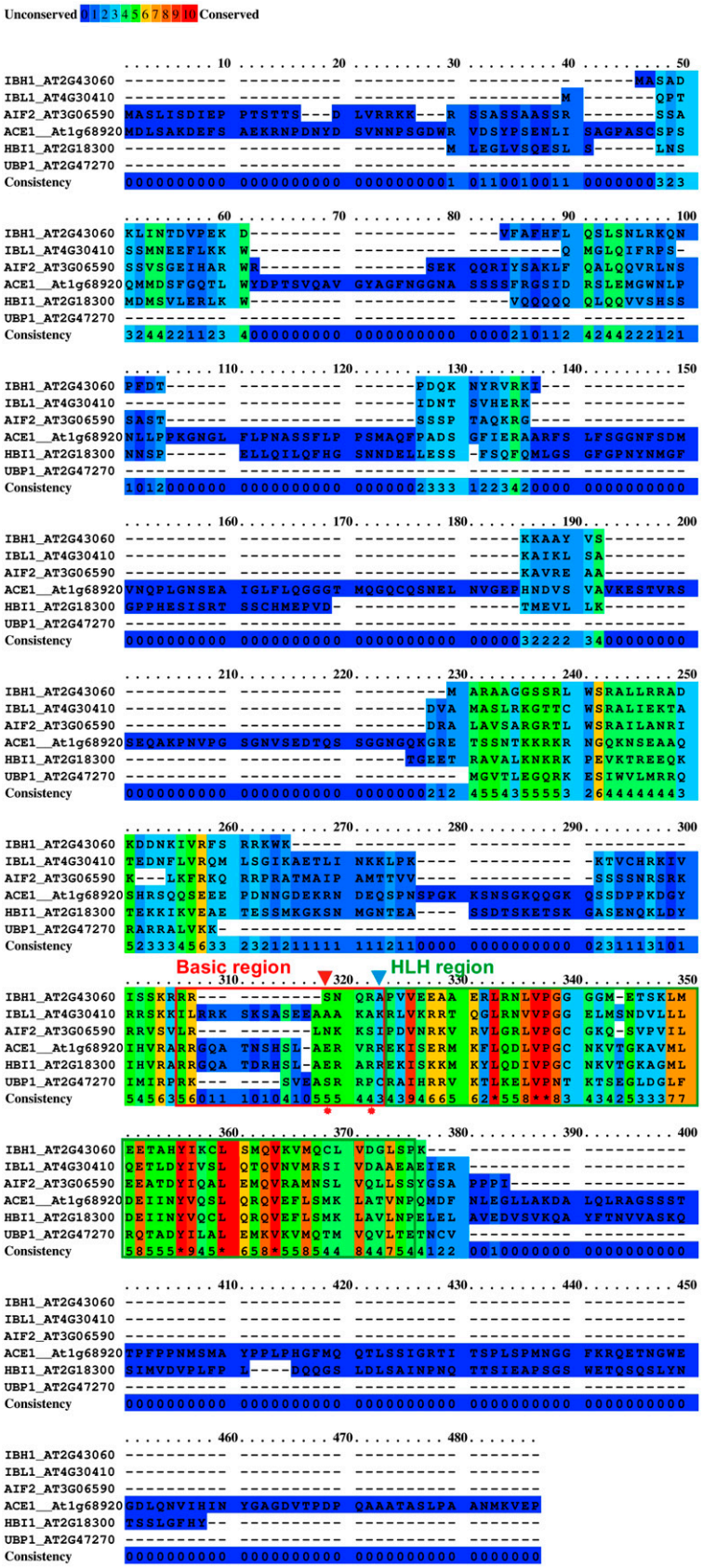

Fig. S1. Alignment of IBH1 and IBL1 with their closest homologs. Color gives the degree of amino acid conservation as indicated by the scale bar. The DNA basic and helix–loop–helix (HLH) regions are in red and green rectangles, respectively. The arrowheads mark the conserved residues in the basic domain required for DNA binding.

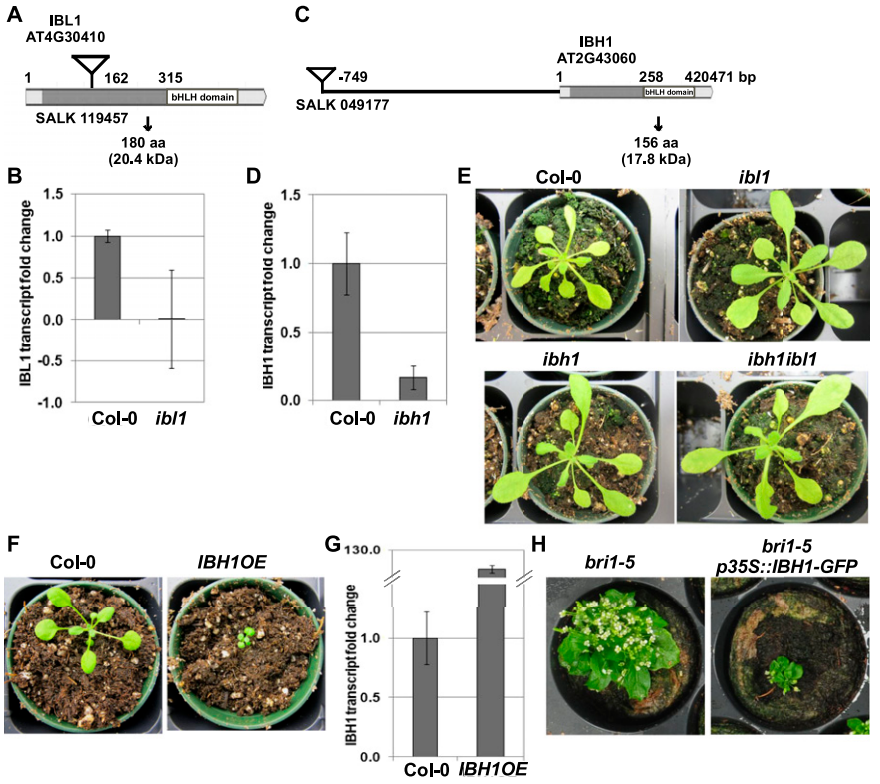

Fig. S2. IBH1 loss- and gain-of-function plants. (*A* and *C*) *IBL1* and *IBH1* gene models and T-DNA insertions. (*B*) Relative *IBL1* transcript level in the *ibl1* mutant and (*D*) relative *IBH1* transcript level in the *ibh1* mutant compared with Columbia-0 (Col-0). $P < 0.01$ relative to Col-0 (Student's *t* test). Seedlings were analyzed at 10 d after sowing (DAS). (*E*) Rosettes of 4-wk-old IBH1 and IBL1 single and double mutants and Col-0. (*F*) Phenotype of *p35S::IBH1-GFP* (*IBH1OE*) plants compared with Col-0 at 21 DAS. (*G*) Relative *IBH1* transcript level in *IBH1OE* plants compared with Col-0 at 10 DAS. $P < 0.0001$ relative to Col-0 (Student's *t* test). (*H*) *bri1-5* transformed with *IBH1OE* construct ($n = 3$; *n*, number of quantitative RT-PCR experiments). Error bars indicate SE.

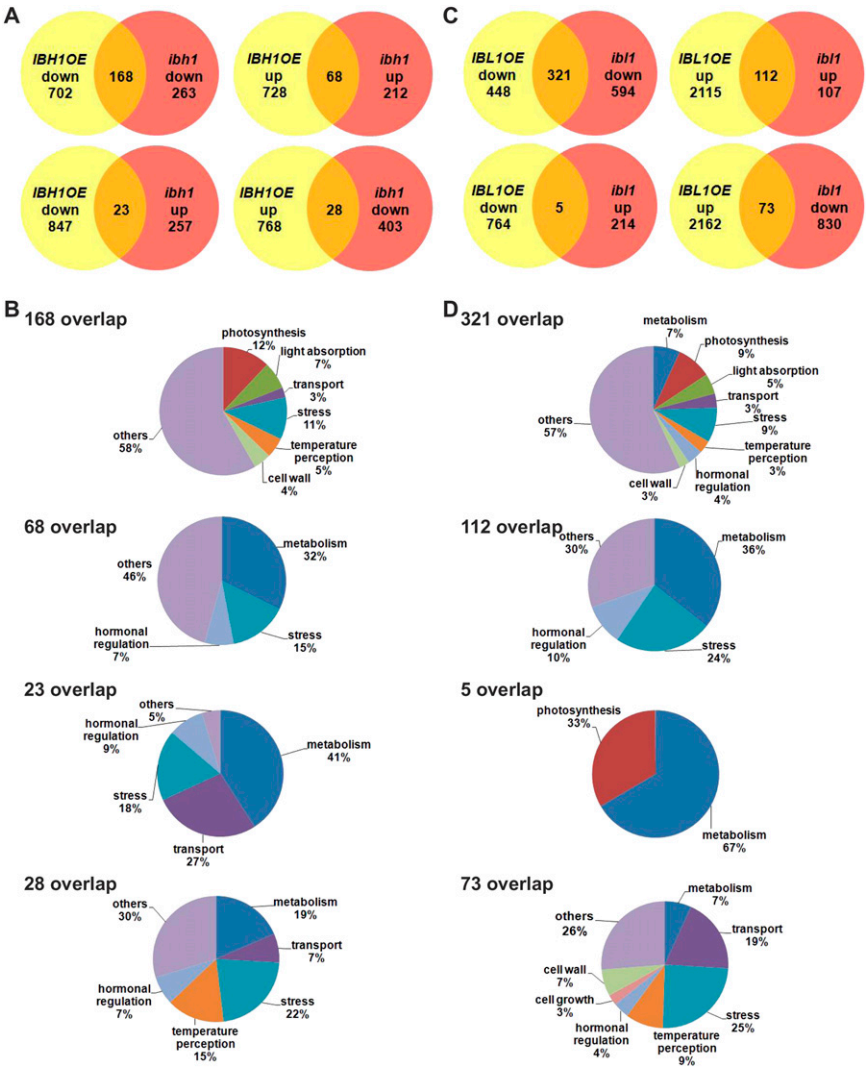

Fig. S3. IBH1- and IBL1-regulated genes. (*A*) Overlaps between genes down- and up-regulated in *IBH1OE* and *ibh1* mutants with statistically significant *P* values [Fisher exact test; 168 ($P = 3.1 \times 10^{-154}$), 68 ($P = 1.0 \times 10^{-48}$), 23 ($P = 1.1 \times 10^{-6}$), and 28 ($P = 1.5 \times 10^{-6}$)]. (*B*) Functional categories of the gene overlaps shown in *A* ($P < 0.05$). (*C*) Overlaps between genes down- and up-regulated in *p35S::IBL1-GFP* (*IBL1OE*) and *ibl1* mutants and respective *P* values [321 ($P = 3.4 \times 10^{-310}$), 112 ($P = 7.3 \times 10^{-73}$), 5 ($P = 0.55$), and 73 ($P = 0.039$)]. (*D*) Functional categories of the gene overlaps shown in *C* ($P < 0.05$).

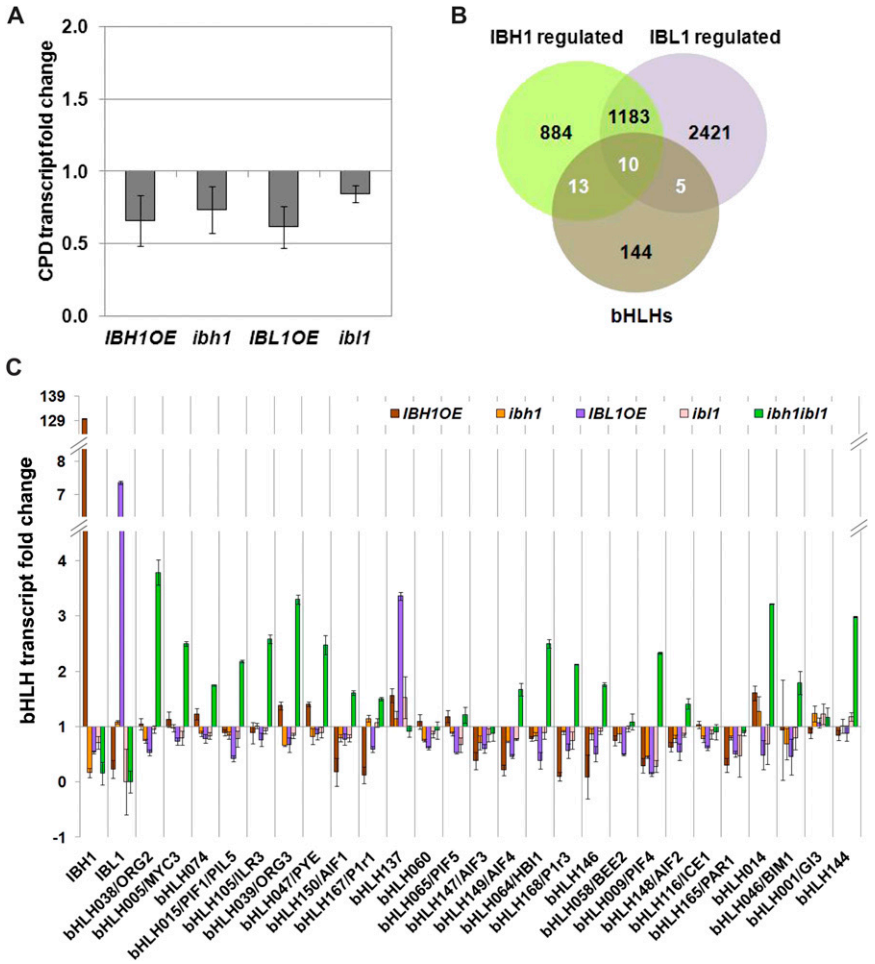

Fig. S4. Genes regulated by IBH1 and IBL1. (*A*) Validation of *CONSTITUTIVE PHOTOMORPHOGENIC DWARF* (*CPD*) expression by quantitative RT-PCR on IBH1 and IBL1 gain- and loss-of-function mutants at 10 DAS. (*B*) Overlap of the differentially expressed genes from the IBH1 and IBL1 RNA-Seq data with the *Arabidopsis* bHLH factors. (*C*) Validation of RNA-Seq expression by quantitative RT-PCR on IBH1 and IBL1 gain- and loss-of-function mutants at 10 DAS. Error bars indicate SE. Three biological and two technical repeats were performed. The significant differences are estimated by Student's *t* test (Dataset S5).

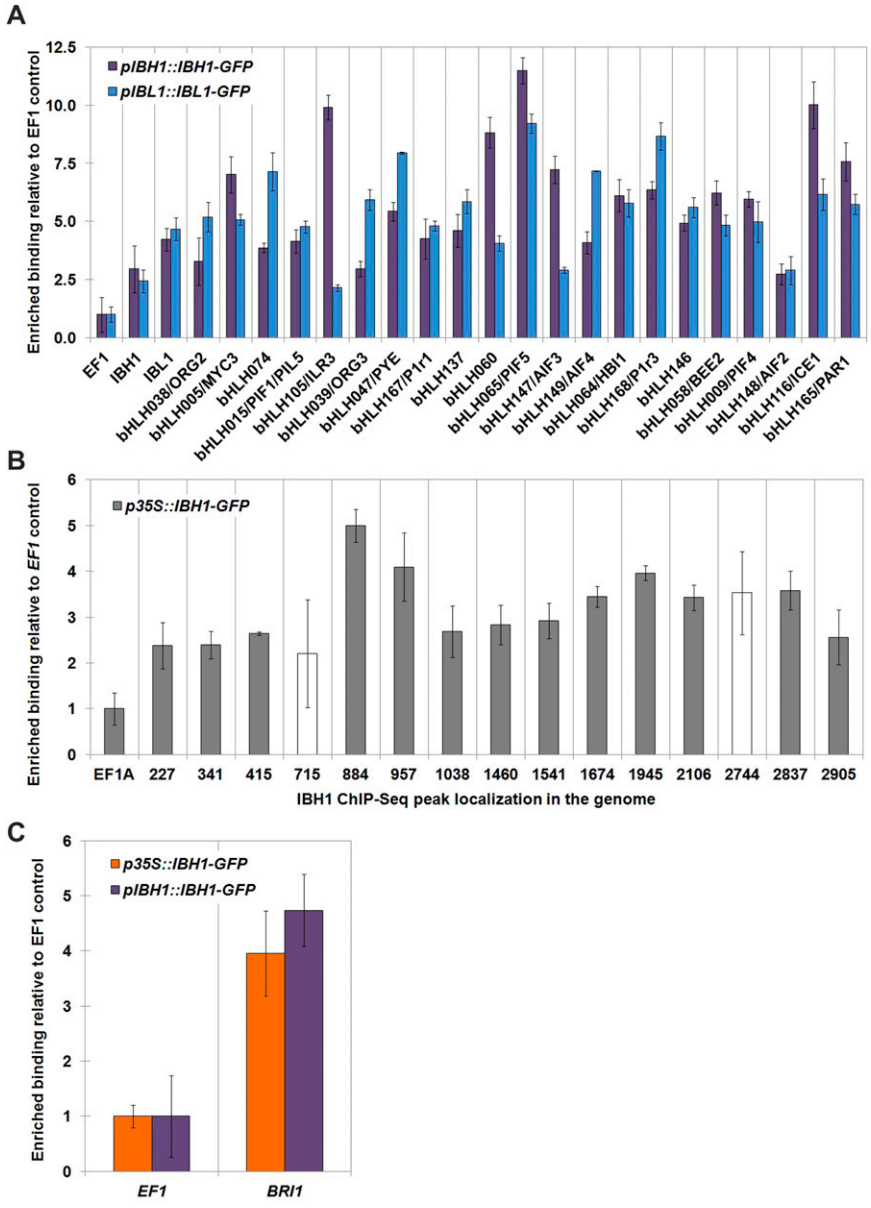

Fig. S5. Validation of the direct bHLH targets of IBH1 and IBL1. (*A*) ChIP-qPCR in transgenic *pIBH1::IBH1-GFP* and *pIBL1::IBL1-GFP* plants at 10 DAS. Four ChIP biological repeats were made, and the average value with standard deviation (SD) is shown. (*B*) ChIP-qPCR validation of random IBH1 binding peaks from the ChIP-Seq analysis relative to the *EF1* control. *p35S::IBH1-GFP* seedlings at 10 DAS were used. Four ChIP biological repeats were made, and the average value with SD is shown. (*C*) ChIP-qPCR validation of IBH1 binding to the *BRI1* promoter relative to the *EF1* control. Both *p35S::IBH1-GFP* and *pIBH1::IBH1-GFP* seedlings at 10 DAS were used. Three ChIP biological repeats were made, and the average value with SD is shown. The significant differences are estimated by Student's *t* test (Dataset S5).

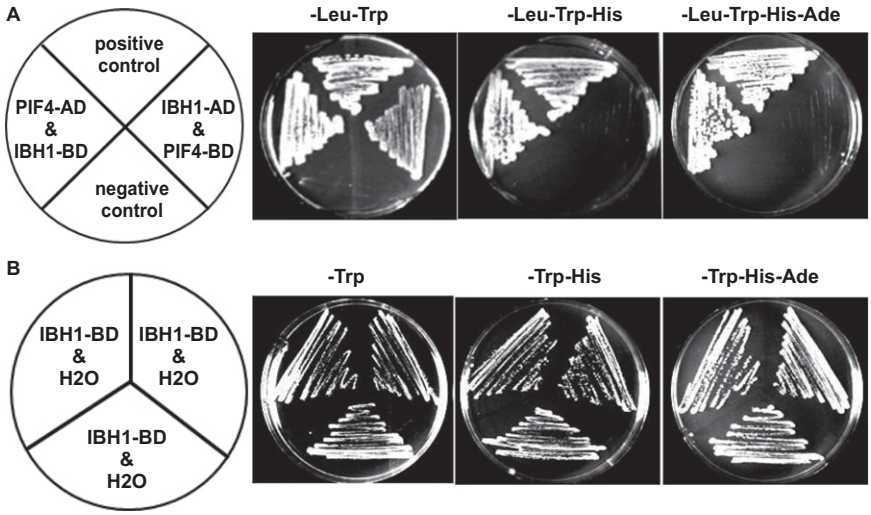

Fig. S6. No interaction of IBH1 and PIF4 in yeast two-hybrid experiments. (*A*) Interactions of IBH1 and PIF4 were tested using each gene in both directions in the pDest-AD and pDest-DB vectors. Growth was observed for Gal4AD-IBH1 and GalDBD-PIF4 but not Gal4AD-PIF4 and GalDBD-IBH1. No growth was visible for untransformed yeast. As a positive control, Gal4AD-AtDIV1 and Gal4DBD-AtDIV1 were used. (*B*) Transformation of GalDBD-IBH1 alone and subsequent screen on selection medium showed growth/self-activation for all colonies tested.

Dataset S1. RNA-Seq data

Dataset S1

This dataset contains the differential expression analysis data sheets in the following tabs. (*A*) RNA-Seq data from *IBH1OE* plants. (*B*) RNA-Seq data from *ibh1* plants. (*C*) RNA-Seq data from *p35S::IBL1-GFP* (*IBL1OE*) plants. (*D*) RNA-Seq data from *ibl1* plants. (*E*) RNA-Seq data from *pifq* plants (1). (*F*) RNA-Seq data from *bzr1-D* plants.

Dataset S2. Lists of IBH1- and IBL1-regulated genes

Dataset S2

This dataset contains the differential expression analysis data sheets in the following tabs. (*A*) List of differentially expressed genes in *IBH1OE* and *ibh1* ($q < 0.05$). (*B*) List of differentially expressed genes in *IBL1OE* and *ibl1* ($q < 0.05$). (*C*) Total lists of genes regulated by *IBH1* and *IBL1*. (*D*) Comparison between the differentially expressed genes in *IBH1OE*, *ibh1*, *IBL1OE*, and *ibl1*.

Dataset S3. IBH1 and IBL1 FunCats

Dataset S3

This dataset contains the differential expression analysis data sheets in the following tabs. (*A*) FunCat of IBH1-, IBL1-, and commonly-regulated genes ($P < 0.05$). (*B*) FunCat of IBH1-regulated genes (overlaps) ($P < 0.05$). (*C*) FunCat of IBL1-regulated genes (overlaps) ($P < 0.05$).

Dataset S4. IBH1 and IBL1 RNA-Seqs compared with published expression data

Dataset S4

This dataset contains the differential expression analysis data sheets in the following tabs. (*A*) Published expression data. (*B*) IBH1 RNA-Seq comparison with published expression data. (*C*) IBL1 RNA-Seq comparison with published expression data. (*D*) IBH1 and IBL1 RNA-Seq comparison with published expression data.

Dataset S5. Transcription factors regulated by IBH1 and IBL1

Dataset S5

This dataset contains differential expression analysis data sheets in the following tabs. (*A*) IBH1- and IBL1-regulated transcription factors based on RNA-Seq data. (*B*) Quantitative RT-PCR validation of the differential expression of bHLH proteins in the IBH1 and IBL1 RNA-Seq data. Fold change of gene expression is shown in *IBH1OE*, *ibh1*, *IBL1OE*, and *ibl1* plants relative to Col-0. SE and *t* test are shown; in green, $P < 0.05$, and in red, $P > 0.05$. IBH1- and IBL1-regulated genes are highlighted in gray. (*C*) bHLH proteins in the IBH1 and IBL1 RNA-Seq data. (*D*) ChIP-qPCR validation of IBH1 and IBL1 direct binding to validated differentially expressed bHLH genes (*B*) and the *BRI1* gene. Enriched IBH1 binding to target gene regulatory regions is shown relative to EF1 control. SD and *t* test are shown; in green $P < 0.05$, and in red, $P > 0.05$. In the case of AIF1, no primers were designed. IBH1 and IBL1 directly regulated bHLH genes are highlighted in gray. (*E*) ChIP-qPCR validation of random IBH1 binding peaks from the ChIP-Seq analysis. Enriched IBH1 binding to random regions in the DNA is shown relative to EF1 control. SD and *t* test are shown; in green, $P < 0.05$, and in red, $P > 0.05$.

Dataset S6. IBH1, PIF4, and BZR1 regulated genes

Dataset S6

This dataset contains the differential expression analysis data sheets in the following tabs. (*A*) Directly regulated genes by IBH1, PIF4, and BZR1. (*B*) FunCat of common target genes ($P < 0.05$).

Dataset S7. Bimolecular fluorescence complementation assays in *N. benthamiana* of the IBH1 and PIF4 interaction

Dataset S7

Dataset S8. List of primers

Dataset S8